Thermodynamic Characterization of Daunomycin–DNA Interactions: Comparison of Complete Binding Profiles for a Series of DNA Host Duplexes†

David P. Remeta,‡,§ Courtney P. Mudd,‖ Robert L. Berger,⊥ and Kenneth J. Breslauer*,‡

Department of Chemistry, Rutgers University, New Brunswick, New Jersey 08903, and Biomedical Engineering and Instrumentation Program, Division of Research Services, and Laboratory of Biophysical Chemistry, National Heart Lung and Blood Institute, National Institutes of Health, Bethesda, Maryland 20892

Received January 19, 1993; Revised Manuscript Received March 10, 1993

ABSTRACT: Using a combination of spectroscopic and calorimetric techniques, we have determined complete thermodynamic binding profiles ($\Delta G°$, $\Delta H°$, and $\Delta S°$) for the complexation of daunomycin to a series of 10 polymeric DNA duplexes. We find the resulting drug binding data to be sensitive to the base composition and sequence of the host duplex, with the binding free energies ranging from −7.5 to −10.8 kcal/mol of bound drug and the binding enthalpies ranging from +4.11 to −10.76 kcal/mol of bound drug at 25 °C. The smaller range in the free energy term reflects the impact of large enthalpy–entropy compensations. We observe that the three synthetic duplexes which exhibit the highest daunomycin binding affinities all contain GC (or IC) base pairs as part of alternating purine/pyrimidine sequence motifs, with these high binding affinities being strongly enthalpy driven at 25 °C. Specific comparisons between the binding profiles for daunomycin complexation with select pairs of host duplexes lead to the following observations: (1) The presence or absence of a major-groove methyl group does not alter daunomycin binding thermodynamics. (2) The presence or absence of a minor-groove amino group does alter daunomycin binding thermodynamics. (3) Duplexes with different base compositions but identical minor-groove functionality exhibit similar daunomycin binding thermodynamics. (4) Homopolymeric duplexes composed of either AT or AU base pairs, but not GC base pairs, exhibit large enthalpy–entropy compensations in their daunomycin binding profiles. We propose interpretations of these and other features of our thermodynamic data in terms of specific daunomycin–DNA interactions deduced from available structural data.

Parallel macroscopic (e.g., thermodynamic) and microscopic (e.g., X-ray, NMR) studies on DNA and its drug complexes yield insights that neither approach alone can provide (Senior et al., 1988; Vesnaver et al., 1989; Marky & Breslauer, 1987b; Jin et al., 1992). In recognition of this advantage, we have pursued, and continue to pursue, a program in which both spectroscopic and calorimetric techniques are being used to characterize thermodynamically the forces that stabilize DNA structures and their drug complexes. We have focused particular attention on systems for which structural data exist so that we can propose correlations between macroscopic and microscopic properties. In this program, we have emphasized the need for complete thermodynamic binding profiles (Breslauer et al., 1987) by demonstrating that enthalpy–entropy compensations can result in drug binding events exhibiting nearly identical binding free energies ($\Delta G°$) despite being driven by entirely different molecular forces ($\Delta H°$ and $\Delta S°$). We also have emphasized the need for direct, model-independent calorimetric measurements of binding enthalpies by demonstrating that indirect, model-dependent van't Hoff analyses can yield a considerable range of ΔH values for the same event (Breslauer et al., 1975; Breslauer, 1986; Remeta et al., 1991). Furthermore, on a practical level, the van't Hoff approach essentially precludes accurate determination of ΔC_p, a parameter accessible by calorimetric measurements (Marky et al., 1985; Breslauer et al., 1992). In light of these considerations, we have used a combination of spectroscopic and calorimetric techniques to determine complete thermodynamic profiles for the DNA binding of daunomycin, a drug for which structural data are available on its DNA complex (Patel & Canuel, 1978; Quigley et al., 1980; Patel et al., 1981; Wang et al., 1987). In fact, we already have described how we have used stopped-flow microcalorimetry to measure directly the binding enthalpies for daunomycin complexation to a family of DNA duplexes (Remeta et al., 1991). Significantly, the enhanced sensitivity of this instrument allowed us to work at monomeric drug concentrations and to evaluate the influence of drug binding density on the binding enthalpy data. We now report complete thermodynamic profiles for the binding of daunomycin to the same series of DNA duplexes. In conjunction with the available structural picture (Quigley et al., 1980; Wang et al., 1987), we interpret the thermodynamic differences we observe in terms of differential daunomycin–DNA interactions due to sequence-dependent structural/conformational differences in the host duplexes.

Daunomycin is a member of the class of glycosidic anthracycline antibiotics that are employed in combination chemotherapy regimens for the treatment of acute leukemia, hematologic malignancies, and a variety of solid tumors in man (Arcamone, 1981; Dorr & Alberts, 1982). This pharmacologically active drug molecule is comprised of two distinct structural domains (Figure 1), a planar aglycone chromophore (daunomycinone) that intercalates between adjacent DNA base pairs and a amino sugar ring (daunosamine) that lies in the minor groove of the helix (Quigley et al., 1980; Wang et

† We gratefully acknowledge the support of the National Institutes of Health (GM23509 and GM34469) to K.J.B.

* To whom all correspondence should be addressed.

‡ Rutgers University.

§ Present address: Laboratory of Biochemistry, Building 3, Room 206, National Heart Lung and Blood Institute, National Institutes of Health, Bethesda, MD 20892.

‖ Biomedical Engineering and Instrumentation Program, Division of Research Services, NIH.

⊥ Laboratory of Biophysical Chemistry, National Heart Lung and Blood Institute, NIH.

0006-2960/93/0432-5064$04.00/0

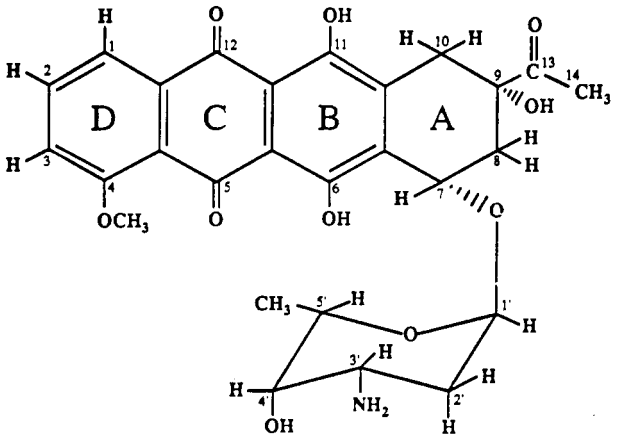

FIGURE 1: Structure of daunomycin.

al., 1987). The cytotoxicity of daunomycin appears to result, in part, from its binding to DNA and consequent inhibition of both the cellular RNA- and DNA-dependent replication and transcription processes (DiMarco et al., 1975; Neidle & Taylor, 1979; Pratt & Ruddon, 1979). In addition to inhibiting nucleic acid synthesis, the anthracyclines cause chromosomal damage by inducing DNA strand breaks (Lown et al., 1977; Ross et al., 1979; Someya & Tanaka, 1979; Gray et al., 1982; Grimmond & Beerman, 1982) and by interacting with chromatin to produce single-stranded regions in nuclear DNA (Center, 1979). Recent evidence suggests that the cytotoxicity elicited by anthracyclines is the consequence of a multistep mechanism which not only includes DNA intercalation but also interaction with the enzyme topoisomerase II, resulting in the formation of topoisomerase II–DNA cleavable complexes (Bodley et al., 1989; Nafziger et al., 1991).

Due to its biological mode of action and its pharmacological activity, the DNA binding properties of daunomycin have been the object of numerous biophysical studies. These studies have focused on either structural or thermodynamic characterizations of daunomycin-DNA interactions. With only a few exceptions, the latter studies have been confined to the determination of binding constants, K_{eq}, and their associated binding free energies, $\Delta G°$ (Neidle & Taylor, 1979; Paar & McNulty, 1979; Chaires et al., 1982, and references cited therein; Walter, 1985). Most of these studies have used Scatchard analyses. Since the Scatchard model formally assumes independent (i.e., noninteracting) binding sites (Scatchard, 1949), the apparent curvature observed in the Scatchard plots generally has been interpreted as reflecting two classes of binding sites with differing affinities for daunomycin (Zunino et al., 1972, 1980; Barthalemy-Clavey et al., 1973; Molinier-Jumel et al., 1978). Subsequent studies (Chaires et al., 1982) have shown that the neighbor exclusion model is more appropriate for analyzing binding data which exhibit marked curvature. Failure to account for neighbor exclusion effects results in an artificially high estimate of K_{eq} and also may result in an erroneous calculation for the number of binding sites (n). Binding constants derived using the neighbor exclusion model yield an intrinsic binding constant of 7.0×10^5 M ($\Delta G° = -8.0$ kcal/mol of bound drug) for the binding of daunomycin to calf thymus DNA in 200 mM Na^+ at 25 °C, with an exclusion parameter of 3–4 base pairs (Chaires et al., 1982). The same study monitored the temperature dependence of the binding constant and calculated a van't Hoff enthalpy of −12.8 kcal/mol and an entropy of −16.8 cal/(deg·mol). A subsequent investigation revealed the enthalpy and entropy of daunomycin–DNA binding to be strongly dependent on the salt concentration. However, due to compensating effects, the binding free energy term remained relatively constant, thereby further underscoring the need for complete thermodynamic binding profiles (Chaires, 1985).

The base sequence specificity of daunomycin also has been the subject of intense study. Initial investigations examined the effect of base composition in natural DNA duplexes on the daunomycin binding affinity. These studies found an increased drug affinity for duplexes with high G-C content (Parr & McNulty, 1979; Chaires et al., 1982). However, since native DNA is a heterogeneous polymer, further elucidation of the sequence specificity of binding required additional studies. To this end, the interaction of daunomycin with synthetic DNA duplexes of defined sequences was investigated by several groups, with conflicting results emerging (Phillips et al., 1978; Chaires, 1983; Graves & Krugh, 1983). The DNA duplexes studied included the alternating copolymers poly[d(AT)]·poly[d(AT)] and poly[d(GC)]·poly[d(GC)] and their homopolymeric sequence isomers poly[d(A)]·poly[d(T)] and poly[d(G)]·poly[d(C)]. Initial studies (Phillips et al., 1978) reported that daunomycin bound with approximately equal affinity to the two purine/pyrimidine sequences and to the G-C homopolymer but less tightly to poly[d(A)]·poly[d(T)]. The apparent number of binding sites varied significantly, however, with the greatest contrast appearing among the A-T polymers.

A subsequent investigation (Chaires, 1983) of the DNA binding properties of daunomycin reported the intrinsic binding constant to decrease in the order poly[d(AT)]·poly[d(AT)] > poly[d(GC)]·poly[d(GC)] > poly[d(G)]·poly[d(C)] > poly[d(A)]·poly[d(T)]. In this study, exclusion parameters of 2.4 and 2.0 were determined for the purine/pyrimidine and purine/purine A-T sequences, 3.6 for the alternating G-C polymer, and 9.8 for poly[d(G)]·poly[d(C)]. These investigators also reported that the ΔT_m values calculated from thermal denaturation experiments correlated reasonably well with the differences observed in the exclusion parameter, thereby providing quantitative support for the measured binding parameters. The results of the latter investigation also are comparable to those reported earlier on the binding of daunomycin to duplexes formed by alternating A-T (i.e., $K_{eq} = 3.2 \times 10^6$; $n = 3.0$) and G-C (i.e., $K_{eq} = 2.4 \times 10^6$; $n = 4.0$) sequences (Graves & Krugh, 1983). A recent study (Xodo et al., 1988) on the binding of daunomycin to an expanded basis set of DNA duplexes reported intrinsic binding constants descending in the order poly[d(Gm^{5}C)]·poly[d(Gm^{5}C)] > poly[d(AT)]·poly[d(AT)] > poly[d(AC)]·poly[d(GT)] > poly[d(IC)]·poly[d(IC)] > poly[d(GC)]·poly[d(GC)] > poly[d(AU)]·poly[d(AU)]. These investigators (Xodo et al., 1988) used the theory of Friedman and Manning (1984) to obtain binding constants, assuming an exclusion site size of two base pairs for each of the host duplexes.

The results of the preceding studies are summarized in the tabulation of equilibrium binding parameters presented in Table I. Owing to the broad range of binding models (i.e., allosteric, neighbor exclusion, Friedman–Manning), experimental methods (i.e., UV/vis, fluorescence, phase partition), and solution conditions (i.e., [Na^+] = 16, 112, 150, 200 mM) employed, one should be cautious about comparisons between these equilibrium binding data. Nevertheless, significant differences are observed in the *relative* binding affinities, as well as in the exclusion parameters measured for the DNA host duplexes, thereby suggesting the need for additional thermodynamic studies.

To address some of the issues noted above, we have pursued a multiparametric approach employing both microcalorimetric

Table I: Summary of Reported Equilibrium Binding Constants and Exclusion Parameters for the Interaction of Daunomycin with Synthetic Deoxypolynucleotides

host DNA polymer	intrinsic binding constant	exclusion parameter (base pairs/drug)	sodium ion concn (mM)	binding model	experimental technique	reference
poly[d(AT)]·poly[d(AT)]	7.6 E+5	2.4	200	neighbor exclusion	fluorescence	Chaires (1983)
	3.2 E+6	3.0	112	allosteric binding	phase partition	Graves and Krugh (1983)
	9.2 E+6	3.0	16	neighbor exclusion	fluorescence	Marky et al. (1984)
	1.2 E+6	2.3	150	neighbor exclusion	UV/vis, fluorescence	Xodo et al. (1988)
	9.4 E+6	2.0	150	Friedman–Manning	UV/vis, fluorescence	Xodo et al. (1988)
poly[d(GC)]·poly[d(GC)]	3.4 E+5	3.6	200	neighbor exclusion	fluorescence	Chaires (1983)
	2.4 E+6	4.0	112	allosteric binding	phase partition	Graves and Krugh (1983)
	8.0 E+5	3.0	16	neighbor exclusion	fluorescence	Breslauer et al. (1987)
	2.4 E+6	3.3	150	neighbor exclusion	UV/vis, fluorescence	Xodo et al. (1988)
	3.4 E+5	2.0	150	Friedman–Manning	UV/vis, fluorescence	Xodo et al. (1988)
poly[d(A)]·poly[d(T)]	2.0 E+4	2.0	200	neighbor exclusion	fluorescence	Chaires (1983)
	3.4 E+5	2.0	16	neighbor exclusion	fluorescence	Breslauer et al. (1987)
poly[d(G)]·poly[d(C)]	1.6 E+5	9.8	200	neighbor exclusion	fluorescence	Chaires (1983)
poly[d(AC)]·poly[d(GT)]	1.7 E+6	2.7	150	neighbor exclusion	UV/vis, fluorescence	Xodo et al. (1988)
	7.1 E+6	2.0	150	Friedman–Manning	UV/vis, fluorescence	Xodo et al. (1988)
poly[d(IC)]·poly[d(IC)]	8.4 E+5	2.7	150	neighbor exclusion	UV/vis, fluorescence	Xodo et al. (1988)
	3.9 E+6	2.0	150	Friedman–Manning	UV/vis, fluorescence	Xodo et al. (1988)
poly[d(AU)]·poly[d(AU)]	4.0 E+5	2.9	150	neighbor exclusion	UV/vis, fluorescence	Xodo et al. (1988)
	1.8 E+6	2.0	150	Friedman–Manning	UV/vis, fluorescence	Xodo et al. (1988)
poly[d(Gm^{5}C)]·poly[d(Gm^{5}C)]	2.3 E+6	2.3	150	neighbor exclusion	UV/vis, fluorescence	Xodo et al. (1988)
	1.4 E+7	2.0	150	Friedman–Manning	UV/vis, fluorescence	Xodo et al. (1988)

and spectroscopic techniques to derive complete thermodynamic binding profiles for a basis set of nine synthetic and one native DNA duplex. Our results are described below.

MATERIALS AND METHODS

Deoxypolynucleotides. The synthetic deoxypolynucleotides employed in this study were obtained from PL Biochemicals (Piscataway, NJ). These DNA polymers were dissolved directly in the 10 mM sodium phosphate buffer system described below. Concentrations for the DNA standard solutions were determined spectrophotometrically at the indicated subscripted wavelengths (nanometers) using the following molar extinction coefficients, ϵ ($M^{-1}\cdot cm^{-1}$), expressed in terms of DNA phosphates: ϵ_{260} of poly[d(AT)]·poly[d(AT)] = 6650, ϵ_{260} of poly[d(A)]·poly[d(T)] = 6000, ϵ_{254} of poly[d(GC)]·poly[d(GC)] = 8400, ϵ_{253} of poly[d(G)]·poly[d(C)] = 7400, ϵ_{258} of poly[d(AC)]·poly[d(GT)] = 6500, ϵ_{258} of poly[d(AG)]·poly[d(CT)] = 5700, ϵ_{260} of poly[d(AU)]·poly[d(AU)] = 6900, ϵ_{257} of poly[d(A)]·poly[d(U)] = 6330, ϵ_{251} of poly[d(IC)]·poly[d(IC)] = 6900, and, ϵ_{260} of salmon testes DNA = 6550.

Daunomycin. The hydrochloride salt of daunomycin was obtained from Sigma Chemical Co. (Milwaukee, WI). Standard solutions of the drug were prepared and used on a daily basis to avoid photodegradation. Concentrations were determined spectrophotometrically by measuring the absorbance of the monomer at 477 nm and using a molar extinction coefficient of 11 500 $M^{-1}\cdot cm^{-1}$. The purity of the daunomycin standards was monitored by thin-layer chromatography. Nuclear magnetic resonance spectra revealed no evidence of drug degradation.

Buffer System. Standard solutions of the DNA polymers and daunomycin were prepared in a buffer consisting of 3.9 mM monobasic sodium phosphate, 6.1 mM dibasic sodium phosphate, and 1.0 mM EDTA. Buffer solutions prepared in this manner typically fell within the pH range of 6.95–6.98, thereby requiring minimal adjustment to pH = 7.00 by addition of microliter aliquots of 1.0 N NaOH. The total sodium ion concentration of this buffer is 15 mM. The buffer was degassed prior to use in all temperature-dependent studies.

Fluorescence Spectroscopy. Binding isotherms for the daunomycin–DNA complexes were constructed by monitoring the change in fluorescence intensity of the free and bound forms of the drug. Corrected fluorescence emission spectra were recorded on a Perkin Elmer MPF-66B fluorescence spectrophotometer operated in the single-wavelength excitation mode at 25 °C. Solutions of the free drug and the drug–DNA complexes were excited at 477 nm and their fluorescence intensity was monitored at 595 nm. Slit widths of 10 nm were employed for both excitation and emission. Measurement of the fluorescence quenching of daunomycin was performed by adding microliter aliquots of the host DNA polymer to a quartz cuvette containing a known amount of drug. Alternatively, separate stock solutions containing equimolar concentrations of daunomycin and the DNA duplex were mixed at varying drug to phosphate ratios, while maintaining a fixed volume of reagents so that the total molar concentration remained constant. The resultant fluorescence data were recorded as a function of the drug binding density and cast in the form of titration curves to determine the exclusion parameter (n) for each host DNA.

Temperature-Dependent UV/Vis Spectroscopy. The thermal stabilities of the drug-free and drug-bound DNA duplexes were measured using temperature-dependent UV/vis spectroscopy. Specifically, absorbance versus temperature melting profiles were determined using a thermoelectrically-controlled Perkin-Elmer 575 programmable UV/vis spectrophotometer interfaced to a Tektronix 4051 computer to facilitate data acquisition, storage, and analysis. Standard solutions of the drug-free duplex and drug-bound complexes at varying degrees of saturation were prepared in the 10 mM sodium phosphate buffer. Samples were placed in 1.0-cm path length quartz cuvettes and heated at a programmed rate of 0.5 °C/min, while the absorbance and temperature were recorded at 20-s intervals. Melting profiles were measured at 260 and 477 nm, with the latter wavelength providing an optical window for monitoring selectively any thermally-induced optical changes in daunomycin. The resultant curves were analyzed by subtracting the absorbance of the buffer solution, normalizing the data, and determining the melting temperatures via established techniques (Breslauer, 1986). Daunomycin–DNA binding constants were calculated as described below from the differences we measured in the melting temperatures

(ΔT_m) of the drug-free (T_m^f) and drug-saturated duplexes (T_m^b).

Calculation of Binding Constants. We have used the formalism developed by Crothers (1968, 1971) and McGhee (1976), and applied by this laboratory (Breslauer et al., 1992; Marky et al., 1985; Snyder et al., 1989), to calculate binding constants from ΔT_m data. The relevant relationship is

$$(1/T_m^f) - (1/T_m^b) = (R/\Delta H°_{h\rightarrow c}) \ln [(1 + K_h a_d)^{B_h}/(1 + K_c a_d)^{B_c}] \quad (1)$$

where T_m^f and T_m^b are the melting temperatures of the drug-free duplex and drug-bound complex, respectively; $\Delta H°_{h\rightarrow c}$ is the helix-to-coil transition enthalpy of the drug-free duplex; K_h and K_c are the apparent drug binding constants to the helix (h) and coiled (c) states, respectively; B_c and B_h are the number of binding sites per base pair of the helix and coiled states, respectively; and a_d is the activity of the drug at the transition temperature, T_m^b, of the drug-bound duplex. Since the binding affinity of daunomycin for single-stranded DNA is negligible compared to that for the duplex state (i.e., $K_c \ll K_h$ and $B_c \leq B_h$), eq 1 may be reduced and rearranged to yield

$$(1/T_m^f) - (1/T_m^b) = (R/n\Delta H°_{h\rightarrow c}) \ln (1 + K_h a_d) \quad (2)$$

where n is the exclusion parameter (i.e., the reciprocal of B_h) expressed as the number of base pairs covered by each drug molecule in the daunomycin–DNA complex. This treatment assumes a simple model in which the binding properties do not depend on the drug-to-DNA ratio. Experimentally, T_m^f and T_m^b are determined from UV melting profiles, $\Delta H°_{h\rightarrow c}$ is measured via differential scanning calorimetry, n is calculated from optical titration curves, and a_d is assumed to be half the total drug concentration at T_m^b. The apparent binding constant (K_h) derived at the transition temperature of the drug-bound duplex is subsequently employed in the standard van't Hoff relationship shown below to calculate the equilibrium binding constant (K_{eq}) at 25 °C:

$$\ln K_{eq} = \ln K_h + \Delta H_b/R(1/T_m^b - 1/298.15) \quad (3)$$

where ΔH_b represents the daunomycin–DNA binding enthalpy determined from stopped-flow microcalorimetric measurements. In this treatment, ΔH_b is assumed to be independent of temperature. In general, care must be taken to ensure that the K_{eq} value derived at saturation by the ΔT_m method and the ΔH_b value measured calorimetrically at lower r values refer to the same binding event.

Differential Scanning Calorimetry. The helix-to-coil transition enthalpy ($\Delta H°_{h\rightarrow c}$) for each of the drug-free DNA host duplexes was determined by differential scanning calorimetry. Standard DNA solutions were prepared in the sodium phosphate buffer system at a concentration of 1.0 mM (expressed in DNA phosphates). The DNA standards and buffer were degassed for approximately 15 min prior to loading both sample and reference cells of a MicroCal MC-2 differential scanning calorimeter (Northampton, MA). Following an equilibration period of 1–2 h, the DNA polymers were heated at a programmed rate of 60 °C/h while the excess heat capacity was recorded as a function of temperature. Comparison of the initial thermogram with subsequent rescans of the polymer revealed complete reversibility of the thermally induced transition for each DNA duplex. The resultant thermograms were integrated and an average value was calculated for the helix-to-coil transition enthalpy of each DNA duplex.

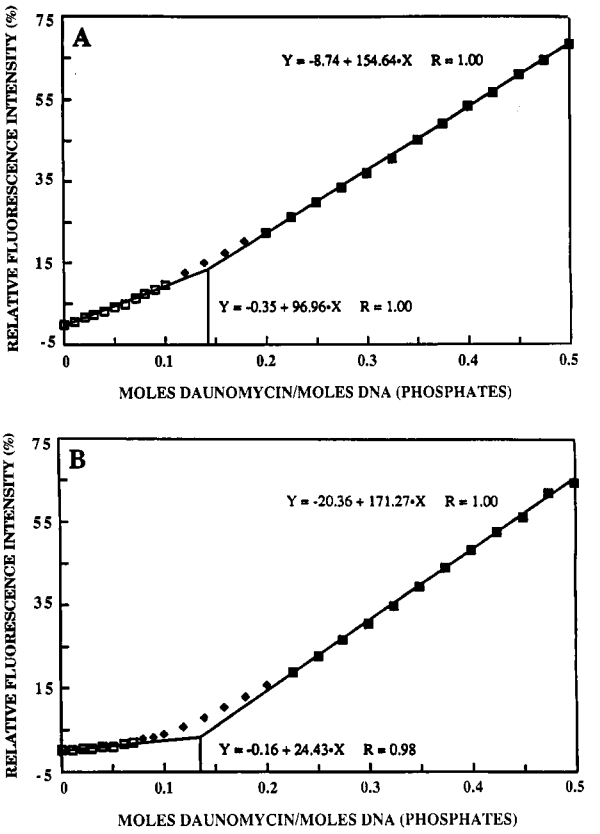

FIGURE 2: Daunomycin–deoxypolynucleotide binding density plots for the host duplexes poly[d(AU)]·poly[d(AU)] in panel A and poly-[d(GC)]·poly[d(GC)] in panel B.

Stopped-Flow Microcalorimetry. Daunomycin–DNA binding enthalpies (ΔH_b) were measured using a differential stopped-flow heat conduction microcalorimeter (Model DS-FC-100, Commonwealth Technology, Inc., Alexandria, VA) developed at the National Institutes of Health (Mudd & Berger, 1988; Mudd et al., 1988). Details regarding design specifications, operational considerations, and discussion of the protocol employed to determine daunomycin–DNA binding enthalpies previously have been described (Remeta et al., 1991). The enhanced differential effective sensitivity of this instrument relative to conventional batch calorimeters enabled direct measurement of daunomycin–DNA binding enthalpies at *monomeric* drug concentrations (i.e., 20 μM), thereby precluding the need to correct for daunomycin self-association. Binding enthalpies were measured at seven different drug binding densities for daunomycin complexation with the 10 DNA host duplexes studied. The stopped-flow microcalorimeter was chemically calibrated at 25.0 °C using the known enthalpies for 1:1 sucrose, hydrochloric acid, and sodium chloride dilutions. An average instrument constant of 1.595 J/(V·s) was determined and employed in all subsequent calculations of the daunomycin–DNA binding enthalpies.

RESULTS

Daunomycin Binding Density. Figure 2 presents optical titration curves obtained from fluorescence quenching measurements of daunomycin complexed with two host duplexes. The data in these plots were evaluated by fitting the straight-line portions that extend from drug to phosphate ratios above and below the DNA lattice saturation. Data points in the immediate vicinity of the saturation point were discarded from the analysis since the plot is curvilinear in this region. The intersection of the two lines furnishes a measure of the

Table II: Summary of Equilibrium Binding Parameters Determined for the Interaction of Daunomycin with Native DNA and Selected Deoxypolynucleotides at 25.0 °C[a]

host DNA polymer	drug-free duplex T_M (°C)	drug-bound complex T_M (°C)	exclusion parameters (base pair/drug)	equilibrium binding constant	binding free energy ($\Delta G°$) (kcal/mol)
poly[d(AT)]·poly[d(AT)]	43.8	80.5	2.8	1.53 E+7	−9.80
poly[d(A)]·poly[d(T)]	51.3	79.1	2.5	1.02 E+6	−8.20
poly[d(GC)]·poly[d(GC)]	97.9	110.6	3.7	2.27 E+7	−10.03
poly[d(G)]·poly[d(C)]	84.6	95.9	3.5	1.01 E+7	−9.56
poly[d(AC)]·poly[d(GT)]	73.3	98.0	3.0	7.99 E+7	−10.78
poly[d(AG)]·poly[d(CT)]	63.8	89.7	3.5	1.39 E+7	−9.75
poly[d(AU)]·poly[d(AU)]	40.6	69.5	3.4	1.34 E+7	−9.72
poly[d(A)]·poly[d(U)]	35.6	60.9	2.5	3.11 E+5	−7.49
poly[d(IC)]·poly[d(IC)]	38.2	74.7	2.5	2.49 E+7	−10.09
salmon testes DNA	67.3	89.9	3.7	4.84 E+7	−10.48

[a] We estimate the uncertainty in the T_m data to be ±0.2 °C and that in the free energy data to be ±0.3 kcal/mol.

stoichiometric ratio for that particular daunomycin–DNA complex. The reciprocal of this value commonly is referred to as the exclusion parameter, *n*, which represents the number of base pairs covered by each drug molecule. The exclusion parameters determined in this manner for each of the DNA host duplexes are summarized in the fourth column of Table II.

Interestingly, we found the magnitude of the upper-line slope in the titration curve to be larger for those host duplexes that exhibited the greater daunomycin binding affinity. Similar behavior has been observed by other investigators who have noted that DNA duplexes containing guanine residues at the intercalation site (e.g., poly[d(AC)]·poly-[d(GT)], poly[d(GC)]·poly[d(GC)], and poly-[d(Gm^5-C)]·poly[d(Gm^{5}C)]) induce nearly total quenching of the daunomycin intrinsic fluorescence, whereas DNA duplexes composed of A-T, A-U, and I-C base pairs effect only partial quenching upon drug binding (Xodo et al., 1988). These empirical observations are supported quantitatively by a comparison between the equilibrium binding constants we have measured (fifth column of Table II) and the upper slopes of our titration curves (data not shown except for Figure 2). In fact, we find the ranking of the daunomycin binding affinity of the DNA duplexes in terms of the slope of the upper line in the titration curves to be in complete concurrence with the thermodynamic ranking based on $\Delta G°$ data.

The site exclusion parameters determined from optical binding plots may be verified by analyzing melting profiles of the drug-free duplexes and drug-saturated complexes. Temperature-dependent UV/vis spectroscopy was employed to monitor the daunomycin-induced thermal stabilization of the DNA duplexes. In most instances, the melting curves were differentiated to facilitate determination of the transition temperatures for both the drug-free (T_m^f) and drug-bound (T_m^b) duplexes. Figure 3 presents such a family of differentiated melting curves acquired at 260 nm for the duplex to single strand transition of poly[d(AT)]·poly[d(AT)] in the absence and presence of daunomycin at the indicated drug to phosphate ratios. The drug-free poly[d(AT)]·poly[d(AT)] duplex melts in a monophasic manner with a narrow transition width and exhibits a T_m^f equal to 43.8 °C (see panel 1 of Figure 3). Addition of nonsaturating amounts of daunomycin increases the thermal stability of the duplex and induces biphasic melting behavior (e.g., panel 2), presumably with drug-free domains in the polymer melting before the thermally stabilized drug-bound domains. The identity of the low- and high-temperature subtransitions was verified further by conducting melting experiments at 477 nm, which provide an optical window for monitoring selectively the thermal disruption of drug-bound regions. At higher drug to phosphate

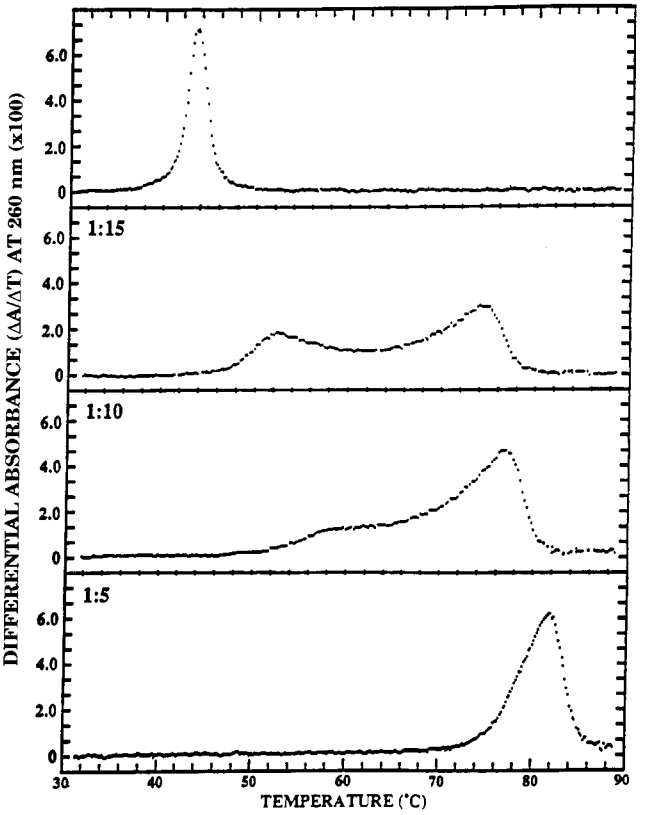

FIGURE 3: Differentiated UV melting profiles for the duplex to single strand transition of poly[d(AT)]·poly[d(AT)] in the absence and presence of daunomycin at selected drug:phosphate ratios.

ratios (e.g., panel 3), the magnitude of the low-temperature transition decreases and that of the high-temperature transition increases. Note that at these intermediate drug to phosphate ratios, the positions of the two subtransitions, as monitored by their respective melting temperatures, are shifted relative to the T_ms of the drug-free and drug-saturated duplexes. As saturation is achieved at a ratio of 1 drug molecule/5 phosphate residues (e.g., panel 4), the drug-bound duplex once again melts in a monophasic manner (e.g., T_m^b = 80.5 °C) but with a greater transition width than that observed for the free duplex. The increase of 36.7 °C in the melting temperature of the drug-saturated versus drug-free duplex reflects the binding-induced thermal stabilization of the daunomycin–poly[d(AT)]·poly[d(AT)] complex, as previously observed (Marky et al., 1983; Breslauer et al., 1987). A complete tabulation of melting temperatures derived from thermal denaturation of the drug-free duplexes and drug-saturated DNA complexes is presented in the first and second columns of Table II.

Determination of Binding Constants and Free Energies of Complexation. Employing the values of T_m^f and T_m^b for the drug-free and drug-bound DNA duplexes, in conjunction with the exclusion parameters (n) obtained from the optical titration curves and the helix-to-coil transition enthalpies ($\Delta H°_{h\rightarrow c}$) of the free duplexes measured via differential scanning calorimetry, we have calculated the apparent drug binding constant, K_h, for each duplex using eq 2. This method for calculating K_h inherently yields a value for the overall drug binding constant at saturation, without resolving individual contributions from complex binding events which may vary with the drug-to-DNA ratio. It should be noted that K_h is calculated at the transition temperature of the drug-saturated duplex, which is dependent on the DNA base composition and sequence. Comparison of daunomycin binding affinities for the DNA host duplexes therefore necessitates application of eq 3 to extrapolate the equilibrium binding constants to a common temperature, in this case 25.0 °C. This extrapolation requires knowledge of the daunomycin–DNA binding enthalpies which, as described above, we have determined using stopped-flow microcalorimetry. The binding enthalpies determined for each of the 10 DNA host duplexes as a function of the drug to phosphate binding density (i.e., D:P = 1:5, 1:7, 1:10, 1:14, 1:20, 1:40, and 1:80) are listed in Table II of our previous paper (Remeta et al., 1991). For the extrapolation of the binding constant to 25 °C (eq 3) we used the binding enthalpy measured under nonsaturating conditions (i.e., r = 0.05), because measurements at this particular drug to phosphate ratio (i.e., D:P = 1:40) require minimal correction for the amount of daunomycin bound per DNA base pair (i.e., $C_B \approx C_T$) since the concentration of free drug is negligible (i.e., $C_F \approx 0$). In addition, the region of $r \geq 0.05$ is characterized by anticooperative binding behavior. Consequently, using ΔH_b at r = 0.05 ensures that competing equilibria associated with cooperative binding events can be disregarded in our calculation of K_{eq}. Substitution into eq 3 of the binding enthalpies for each of the daunomycin–DNA complexes yields the respective equilibrium binding constants and binding free energies summarized in the last two columns of Table II. Significantly, the binding free energies we calculate by this "ΔT_m method" are in good agreement with those we have measured more conventionally by analysis of fluorescence quenching data at much lower drug binding densities (Remeta, 1990; Breslauer et al., 1992). This agreement gives us confidence in our use of the ΔT_m method to calculate the free energy values reported here.

Complete Thermodynamic Binding Profiles. Combining of the calorimetrically measured binding enthalpies reported in our previous paper (Remeta et al., 1991) with the spectroscopically determined binding free energies described herein allows us to calculate the binding entropies for each of the drug–DNA systems studied using the standard thermodynamic relationship:

$$\Delta G° = \Delta H° - T\Delta S°$$

The resulting data at 25 °C are summarized in Table III.

In the sections that follow, we compare and discuss these various binding profiles in an effort to develop insights into the molecular origins of our thermodynamic data.

DISCUSSION

The DNA Binding Profiles of Daunomycin Vary with the Base Composition and Sequence of the Host Duplex. The data in Table III reveal the thermodynamics of daunomycin–DNA binding to be quite sensitive to the base composition and sequence of the host duplex. To be specific, the binding free energies range from −7.49 to −10.78 kcal/mol, which corresponds to a binding constant range of 3.11×10^5 to 7.99×10^7 at 25 °C. Even more impressive is the spread in the binding enthalpies, which range from +4.11 to −10.76 kcal/mol. Even if one excludes the two "aberrant" homopolymeric duplexes, the spread in the binding enthalpies is still substantial (−6.18 to −10.76 kcal/mol).

Table III: Complete Thermodynamic Binding Profiles Derived for the Interaction of Daunomycin with Native DNA and Selected Deoxypolynucleotides at 25 °C[a]

host DNA polymer	$\Delta G°$ (kcal/mol)	$\Delta H°$ (kcal/mol)	$\Delta S°$ [cal/(mol·deg)]	$T\Delta S°$ (kcal/mol)
poly[d(AT)]·poly[d(AT)]	−9.80	−6.18	12.14	3.62
poly[d(A)]·poly[d(T)]	−8.20	+3.54	39.37	11.74
poly[d(GC)]·poly[d(GC)]	−10.03	−9.40	2.13	0.63
poly[d(G)]·poly[d(C)]	−9.56	−7.10	8.24	2.46
poly[d(AC)]·poly[d(GT)]	−10.78	−10.76	0.06	0.02
poly[d(AG)]·poly[d(CT)]	−9.75	−5.87	13.00	3.88
poly[d(AU)]·poly[d(AU)]	−9.72	−6.31	11.44	3.41
poly[d(A)]·poly[d(U)]	−7.49	+4.11	38.92	11.60
poly[d(IC)]·poly[d(IC)]	−10.09	−6.86	10.83	3.23
salmon testes DNA	−10.48	−9.52	3.23	0.96

[a] We estimate the average uncertainty in the binding enthalpies to be ~±0.34 kcal/mol, so the final digit is not significant for all data in the table. Individual uncertainties for each enthalpy value are given in Remeta et al. (1991).

It is interesting to note that the three synthetic duplexes with the highest binding affinities all contain alternating purine/pyrimidine sequences and GC (or IC) base pairs. Furthermore, in all three cases, the high binding affinities are strongly enthalpy-driven. It should be noted that the one natural DNA duplex studied exhibits a daunomycin thermodynamic binding profile similar to that found when poly[d(GC)]·poly[d(GC)] and poly[d(AC)]·poly[d(GT)] served as the host duplexes. This result may suggest that daunomycin binding to salmon testes DNA involves interactions with sites similar to those found in these two synthetic DNA duplexes. In this connection, it is of interest to note that footprinting studies by Chaires et al. (1987) on natural DNA duplexes reveal that daunomycin selectively protects GC-rich sequences, with adjacent GC base pairs being a particular feature of such protected domains. Our thermodynamic binding profiles are consistent with these footprinting results. The Chaires et al. (1987) study further suggests that the optimal daunomycin binding site may be a triplet sequence comprising AT base pairs at the 5′ position flanked by two contiguous GC base pairs of variable sequence. Studies using poly[d(AGC)]·poly[d(GCT)] and poly[d(AGG)]·poly[d(CCT)] as host duplexes may allow us to isolate and define the thermodynamic contribution for daunomycin binding to this class of putative optimal sites. In the sections that follow, we focus on specific comparisons between the binding profiles we have measured for daunomycin complexation with select pairs of host DNA duplexes. These comparisons are designed to provide us with insight(s) into the molecular origins of our thermodynamic data.

A Major-Groove Methyl Group Does Not Alter the Daunomycin Binding Thermodynamics. The poly[d(AT)]·poly[d(AT)] and poly[d(AU)]·poly[d(AU)] duplexes formally differ by the presence or absence of a methyl group on the pyrimidine base (see Figure 4). This methyl group projects into the major groove of B-form double helices. Inspection of the data in Table III reveals that these two duplexes exhibit essentially equivalent thermodynamic profiles

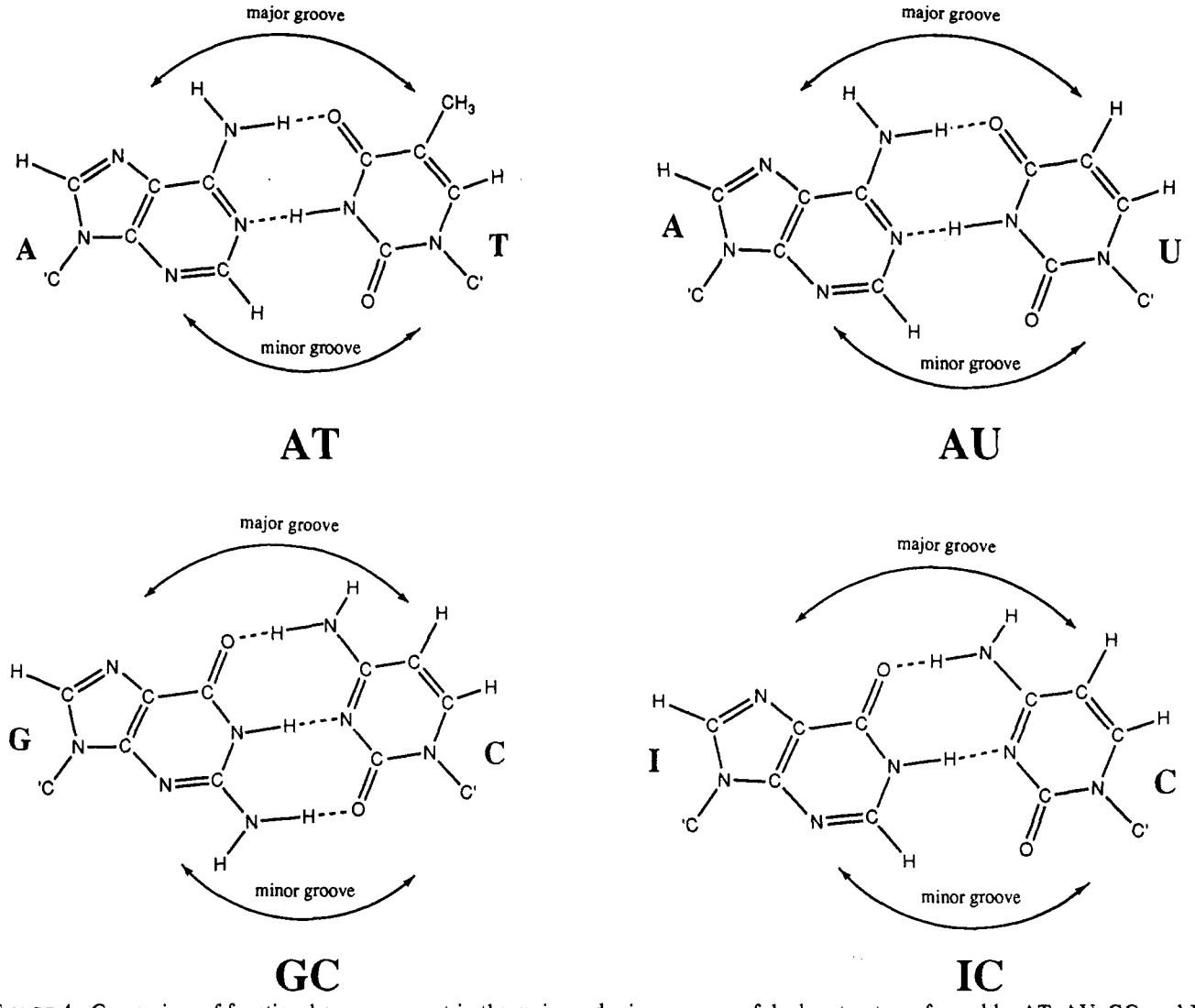

FIGURE 4: Comparison of functional groups present in the major and minor grooves of duplex structures formed by AT, AU, GC, and IC base pairs.

for daunomycin binding. In the absence of fortuitous compensations, this equivalence suggests that the events associated with daunomycin–DNA complexation do not directly or indirectly involve interactions with the major groove, particularly the domain into which the methyl group projects. This thermodynamically based conclusion is consistent with the available structural data (Quigley et al., 1980; Wang et al., 1987), which reveal that the anthracycline ring system intercalates and the pendant sugar ring resides in the minor groove. Even if the intercalated ring system were to protrude partly into the major groove, our data suggest that it does not thermodynamically sense any difference in this domain due to the presence or absence of the pyrimidine methyl group. A qualitatively similar set of conclusions can be reached by comparison of the daunomycin binding profiles for complexation with the poly[d(A)]·poly[d(T)] and poly[d(A)]·poly[d(U)] duplexes. However, we and others have proposed that ligand binding to these two homopolymeric duplexes also involves a binding-induced helix-to-helix change in conformation/hydration, thereby rendering quantitative comparisons of these binding data more complex (Marky et al., 1985; Wilson et al., 1985; Breslauer et al., 1987; Herrera & Chaires, 1989).

At the beginning of the preceding discussion, we qualified our interpretation of the equivalence of the observed thermodynamic binding profiles, with the caveat "In the absence of fortuitous compensations, ...". In general, such a statement is required whenever one attempts to interpret macroscopic thermodynamic data in terms of specific microscopic molecular interactions. In particular, for the reasons described below, we judge this disclaimer to be reasonable for comparisons between the daunomycin binding profiles of the two host duplexes under consideration.

Intercalation of the anthracycline ring system into the host duplexes involves two events: intercalation-induced unstacking of the existing d(AT)/d(TA) and d(AU)/d(UA) nearest-neighbor interactions and compensatory stacking of the exogenous anthracycline ring system with the previously stacked endogenous base pairs. We judge the first unstacking event to be thermodynamically equivalent for the two host duplexes since our differential scanning calorimetric measurements reveal the ligand-free poly[d(AT)]·poly[d(AT)] and poly[d(AU)]·poly[d(AU)] duplexes to exhibit essentially identical thermodynamic melting profiles (Chou, 1990). By extension, with regard to the second event, one also might propose a thermodynamic equivalence for the stacking of the exogenous intercalating ring system with the endogenous d(AT) and d(AU) base pairs. In the absence of the above circumstances, one would be forced to evoke extensive fortuitous compensations between the thermodynamics of all intercalative and nonintercalative interactions (e.g., the sugar ring of the drug and the minor groove of DNA), to rationalize the thermodynamic equivalence we observe for

daunomycin binding to the poly[d(AT)]·poly[d(AT)] and poly[d(AU)]·poly[d(AU)] duplexes. Without evidence that demands such an interpretation of greater complexity, we judge our microscopic interpretation of the thermodynamic data to represent a reasonable framework for further discussion which is consistent with the available structural picture.

A Minor-Groove Amino Group Alters the Daunomycin Binding Thermodynamics. The poly[d(GC)]·poly[d(GC)] and poly[d(IC)]·poly[d(IC)] duplexes formally differ by the presence or absence of an amino group in the minor groove, while the functional groups and the hydrogen-bonding pattern in the major groove remains the same (see Figure 4). Inspection of the data in Table III reveals the thermodynamic driving forces ($\Delta H°$, $\Delta S°$) for daunomycin complexation with these two duplexes to be quite different, despite the fact that an enthalpy–entropy compensation results in essentially identical binding free energies ($\Delta G°$). It is of interest to interpret the differential binding enthalpy ($\Delta\Delta H$) we measure (approximately 2.5 kcal/mol of bound daunomycin) in terms of the available structural data. As noted earlier, X-ray (Quigley et al., 1980; Wang et al., 1987) and NMR data (Remeta, 1990; Remeta et al., 1987a,b; D. J. Patel et al., unpublished results) reveal that daunomycin binding involves intercalation of the anthracycline moiety, with the sugar residue lying in the minor groove. Further, when a guanine residue is adjacent to the intercalation site, the structural data suggest that the oxygen of the C-9 hydroxyl group of the daunomycin A ring forms a hydrogen bond with a hydrogen atom of the N2 exocyclic amino group of guanine. Since this amino group is missing in inosine, daunomycin binding to the poly[d(IC)]·poly[d(IC)] duplex formally will have one less drug–DNA hydrogen bond in the minor groove than binding to the poly[d(GC)]·poly[d(GC)] duplex. Implicit in this argument is the reasonable assumption that the general motif of drug binding remains the same for these two duplexes. On the basis of this reasoning, one is tempted to ascribe the observed reduction in favorable daunomycin binding enthalpy to poly[d(IC)]·poly[d(IC)] relative to poly[d(GC)]·poly[d(GC)] ($\Delta\Delta H$ = 2.5 kcal/mol of bound daunomycin) to the loss of this hydrogen bond, a value which falls within current estimates for such an interaction (Freier et al., 1986; Kim & Baldwin, 1990; Shirley et al., 1992). However, this interpretation of the data implicitly assumes that all other daunomycin–DNA intractions remain enthalpically equivalent for the poly[d(IC)]·poly[d(IC)] and poly[d(GC)]·poly[d(GC)] duplexes. We have several reasons for making this assumption. First, the two drug-free duplexes exhibit identical transition enthalpies (Chou, 1990). In the absence of fortuitous compensations, this result suggests IC/CI and GC/CG stacking interactions to be enthalpically equivalent. By extension, we again reason the enthalpic contribution from intercalation-induced DNA base unstacking and concomitant anthracycline–DNA stacking interaction to be similar for poly[d(IC)]·poly[d(IC)] and poly[d(GC)]·poly[d(GC)], thereby allowing us to focus our attention on other drug–DNA interactions to rationalize the molecular origins of the thermodynamic differences we observe. In addition to the daunomycin O9–guanine N2 H-bond noted above, the structural picture also reveals a second hydrogen bond between the hydrogen of the same C-9 daunomycin hydroxyl group (which for convenience will be called H9) and the ring N3 of guanine in the minor groove (Quigley et al., 1980; Wang et al., 1987). Significantly, inosine also has a N3 atom positioned in the same location within the minor groove as the N3 of guanine. Thus, by analogy we reason that this daunomycin H9–DNA N3 minor-groove hydrogen bond will exist in the daunomycin–DNA complex when either poly[d(IC)]·poly[d(IC)] or poly[d(GC)·poly[d(GC)] serves as the host duplex, although we do not demonstrate these two H9–N3 H-bonds to be of comparable strength.

In summary, on the basis of the available structural picture and the reasonable inferences and assumptions described above, we ascribe our measured differential daunomycin binding enthalpy of ~2.5 kcal to the poly[d(GC)]·poly[d(GC)] and poly[d(IC)]·poly[d(IC)] duplexes to the loss of the daunomycin C-9 hydroxyl–N2 guanine minor-groove hydrogen bond which is present when poly[d(GC)]·poly[d(GC)] acts as the host duplex but absent when the poly[d(IC)]·poly[d(IC)] duplex is the host. However, independent of the validity of this molecular interpretation, our data reveal a substantial quantitative difference in the enthalpic and entropic driving forces which control the binding of daunomycin to the poly[d(GC)]·poly[d(GC)] and the poly[d(IC)]·poly[d(IC)] duplexes. Significantly, these intriguing thermodynamic differences would have been missed if one only measured the corresponding binding free energies, which are essentially equal due to enthalpy–entropy compensations.

A Homopurine·Homopyrimidine DNA Duplex and Its Corresponding Alternating Purine/Pyrimidine Duplex Exhibit Different Daunomycin Binding Thermodynamics. The poly[d(AG)]·poly[d(CT)] and poly[d(AC)]·poly[d(GT)] duplexes differ by the fact that in the former duplex the purine and pyrimidine residues are segregated on separate strands while in the latter duplex they alternate along each strand. As a result, each duplex contains a different set of potential intercalation sites for daunomycin. This feature is reflected in the data obtained from DSC measurements on these two duplexes, which reveal that poly[d(AC)]·poly[d(GT)] exhibits a transition enthalpy per nearest neighbor which is nearly 3 kcal larger (more endothermic) than that of poly[d(AG)]·poly[d(CT)] (Chou, 1990). This feature of thermodynamically different intercalation sites is reflected further in the significantly different daunomycin binding profiles we measure for these two duplexes. Inspection of the data in Table III reveals that the differences are particularly apparent in the enthalpy and entropy terms, with the net effect in the free energy term being somewhat dampened by enthalpy–entropy compensations.

The substantially greater binding enthalpy we measure for complexation of daunomycin to poly[d(AC)]·poly[d(GT)] is consistent with intercalation-induced unstacking of nearest-neighbor interactions in a manner that is not fully compensated for by the resulting stacking interactions between the DNA bases and the anthracycline ring system of the drug. Clearly, part of these differences also may reflect differential minor-groove interactions of the sugar moiety. Further studies on more diverse duplex sequences are required to resolve and to define these various potential contributions to the thermodynamic data.

Duplexes with Identical Minor Grooves Exhibit Similar Daunomycin Binding Thermodynamics. The minor-groove domains of the poly[d(AT)]·poly[d(AT)] and poly[d(IC)]·poly[d(IC)] duplexes are equivalent with respect to the number, type, and disposition of functional groups (see Figure 4). Specifically, the minor groove of both duplexes present in a topologically equivalent fashion a purine ring nitrogen and C-H hydrogen, as well as a pyrimidine carbonyl group. By contrast, the disposition of the functional groups within the major groove of these two duplexes is reversed. Inspection of the relevant data in Table III reveals very similar, albeit not

identical, thermodynamic profiles for daunomycin binding to these two duplexes. This thermodynamic similarity superficially appears to support the structural picture in which the C-9 hydroxyl group of daunomycin hydrogen bonds to the N3 of the purine residue, a site present and similarly disposed in the minor grooves of both poly[d(AT)]·poly[d(AT)] and poly[d(IC)]·poly[d(IC)]. The quantitative differences we observe may simply reflect differences in the electron density maps of AT and IC base pairs, which in turn would alter the strengths of the hydrogen bond. In this connection, we previously have observed a similar thermodynamic effect for the binding of netropsin, a nonintercalating, minor-groove-directed ligand, to the same two duplexes (Marky & Breslauer, 1987b).

As just acknowledged, this microscopic interpretation of the macroscopic data is somewhat superficial since we are implicitly assuming that the thermodynamic contribution arising from anthracycline ring intercalation is similar for both duplexes. The free energy component of this assumption may be reasonable since poly[d(IC)]·poly[d(IC)] and poly[d(AT)]·poly[d(AT)] exhibit very similar $\Delta G°$ values for unstacking (Chou, 1990). By contrast, the enthalpic component of this assumption is less reasonable since the two duplexes exhibit very different transition enthalpies (Chou, 1990). Perhaps the *net* effect of intercalation-induced DNA unstacking and drug–DNA stacking compensate each other in a manner that leads to similar enthalpic contributions for daunomycin intercalation into IC/CI and AT/TA stacking sites. To evaluate this possibility, we are conducting corresponding calorimetric studies on the DNA binding of an aglycone derivative of daunomycin which lacks the hydroxyl group at the C-9 position as well as the sugar ring, thereby allowing us to isolate the thermodynamic contribution of the intercalation event. In the interim, one should focus on our experimental results rather than on the details of the proposed molecular interpretations. Nevertheless, it is intriguing to note that the three B-form duplexes which possess identical minor grooves [poly[d(AT)]·poly[d(AT)], poly[d(AU)]·poly[d(AU)], and poly[d(IC)]·poly[d(IC)]] but different major grooves all exhibit similar daunomycin thermodynamic binding profiles. By contrast, two duplexes with different minor grooves but identical major grooves [poly[d(GC)]·poly[d(GC)] and poly[d(IC)]·poly[d(IC)]] exhibit considerable differences in the thermodynamic driving forces for daunomycin binding. In the aggregate, these thermodynamic differences are consistent with the structural picture which reveals that, in addition to intercalation of the anthracycline ring system, specific daunomycin–DNA interactions are expressed in the minor groove.

Daunomycin Binding to All-AT or All-AU Homopolymeric Duplexes Exhibits Enthalpy–Entropy Compensations That Are Absent When the All-GC Homopolymeric Duplex Acts as the Host. Inspection of the data in Table III reveals daunomycin binding to the alternating copolymer poly[d(AT)]·poly[d(AT)] duplex to be strongly enthalpy-driven at 25 °C. By contrast, daunomycin binding to the corresponding homopolymer poly[d(A)]·poly[d(T)] duplex is totally entropy-driven at 25 °C, with an enthalpy contribution that actually is inhibitory (endothermic). By measuring the binding enthalpy at different temperatures, we have shown that these observations are not a trivial function of the temperature of comparison, in this case, 25 °C. Due to enormous enthalpy–entropy compensations, however, the large difference in binding enthalpy for these two duplexes is substantially dampened in the binding free energy term. This laboratory (Marky et al., 1985; Breslauer et al., 1987) and others (Wilson et al., 1985; Herrera & Chaires, 1989) previously have reported such behavior for these two duplexes and have interpreted this phenomenon in terms of a binding-induced change in conformation/hydration for the poly[d(A)]·poly[d(T)] homopolymeric duplex. Further inspection of the data in Table III reveals that this aberrant thermodynamic daunomycin binding profile also is observed when poly[d(A)]·poly[d(U)] serves as the homopolymeric host duplex. This new result shows that the presence or absence of a pyrimidine methyl group in the major groove does not alter the property (or properties) of the homopolymeric duplex that gives rise to this aberrant behavior. By contrast, relative to its corresponding all-GC, alternating copolymeric duplex poly[d(GC)]·poly[d(GC)], the all-GC, homopolymeric duplex poly[d(G)]·poly[d(C)] does not exhibit this unusual behavior. This new observation suggests that the unique properties of the all-AT (or AU) homopolymeric duplexes which give rise to their aberrant thermodynamic daunomycin binding profiles are not manifest in the all-GC homopolymer duplex poly[d(G)]·poly[d(C)]. Such a conclusion is consistent with available structural and hydration data which suggest that, in contrast to the all-GC homopolymeric duplex, the all-AT homopolymeric duplex adopts a non-B-form conformation which is more highly hydrated.

CONCLUDING REMARKS

We have reported complete thermodynamic binding profiles for the complexation of daunomycin with nine synthetic and one natural DNA duplexes. We found that the binding profiles exhibit substantial differences for duplexes with different base compositions and sequences. We noted that three duplexes which possess functionally equivalent minor grooves but different major grooves exhibit similar thermodynamic binding profiles. By contrast, we found that two duplexes with different minor grooves but functionally equivalent major grooves exhibit considerable differences in the thermodynamic driving forces for daunomycin binding. We observed that these thermodynamic differences are consistent with the structural picture, which reveals the presence of specific drug–DNA interactions in the minor groove but not in the major groove. In fact, we used the structural data to interpret the quantitative thermodynamic differences for daunomycin binding to one duplex versus another in terms of the existence or loss of particular drug–DNA hydrogen bonds, thereby underscoring the value of parallel structural and thermodynamic studies. Future studies on systematically altered drug and DNA analogues should allow us to define further the thermodynamic contributions that specific daunomycin–DNA interactions make to the binding affinity and specificity of this pharmacologically active ligand. As previously emphasized (Marky & Breslauer, 1987b; Breslauer et al., 1988), such information is needed for developing a rational approach to drug design.

REFERENCES

Arcamone, F. (1981) *Med. Chem. (Academic Press) 17*, 1.
Barthalemy-Clavey, V., Maurizot, J. C., & Sicard, P. J. (1973) *Biochimie 55*, 859–868.
Bodley, A., Liu, L. F., Israel, M., Seshadri, R., et al. (1989) *Cancer Res. 49*, 5969–78.
Breslauer, K. J. (1986) in *Thermodynamic Data for Biochemistry and Biotechnology* (Hinz, H., Ed.) pp 402–427, Springer-Verlag, New York.
Breslauer, K. J., Sturtevant, J. M., & Tinoco, I., Jr. (1975) *J. Mol. Biol., 99*, 549–565.
Breslauer, K. J., Remeta, D. P., Chou, W. Y., Ferrante, R., Curry, J., Zaunczkowski, D., Snyder, J. G., & Marky, L. A. (1987)

Proc. Natl. Acad. Sci. U.S.A. 84, 8922–8926.
Breslauer, K. J., Ferrante, R., Curry, J., Zaunczkowski, D., Youngquist, R. S., Dervan, P. B., & Marky, L. A. (1988) in *Structure & Expression, Vol. 2, DNA and its Drug Complexes* (Sarma, M. H., & Sarma, R. H., Eds.) pp 273–290, Adenine Press, Guilderland, NY.
Breslauer, K. J., Freire, E., & Straume, M. (1992) *Methods Enzymol. 211*, 533–567.
Center, M. S. (1979) *Biochem. Biophys. Res. Commun. 89*, 1231–1238.
Chaires, J. B. (1983) *Biochemistry 22*, 4204–4211.
Chaires, J. B. (1985) *Biopolymers 24*, 403–419.
Chaires, J. B. (1990) *Biophys. Chem. 35*, 191–202.
Chaires, J. B., Dattagupta, N., & Crothers, D. M. (1982) *Biochemistry 21*, 3933–3940.
Chaires, J. B., Fox, K. R., Herrera, J. E., Britt, M., & Waring, M. J. (1987) *Biochemistry 26*, 8227–8235.
Chaires, J. B., Herrera, J. E., & Waring, M. J. (1990) *Biochemistry 29*, 6145–53.
Chou, W.-Y. (1990) Ph.D. Thesis, Rutgers University, New Brunswick, NJ.
Crothers, D. M. (1968) *Biopolymers 6*, 575–584.
Crothers, D. M. (1971) *Biopolymers 10*, 2147–2160.
DiMarco, A., Arcamone, F., & Zunino, F. (1975) in *Antibiotics, Mechanism of Action of Antimicrobial and Antitumor Agents* (Corcoran, J. W., & Hahn, F. E., Eds.) pp 101–128, Springer-Verlag, Berlin.
Dorr, R. T., & Alberts, D. S. (1982) in *Current Concepts in the Use of Doxorubicin Chemotherapy* (Jones, S. E., Ed.) pp 1–20, Adria Labs, Graphiche Milani, Italy.
Freier, S. M., & Sugimoto, N., Sinclair, A., Alkema, D., Neilson, T., Kierzek, R., Caruthers, M. H., & Turner, D. H. (1986) *Biochemistry 25*, 3214–3219.
Friedman, R. A. G., & Manning, G. S. (1984) *Biopolymers 23*, 2671–2714.
Gabby, E. J., Grier, D., Fingerle, R. E., Reimer, R., Levy, R., Pearce, S. W., & Wilson, W. D. (1976) *Biochemistry 15*, 2062–2070.
Graves, D. E., & Krugh, T. R. (1983) *Biochemistry 22*, 3941–3947.
Gray, P. J., Phillips, D. R., & Wedd, A. G. (1982) *Photochem. Photobiol. 36*, 49–57.
Grimmond, H. E., & Beerman, T. (1982) *Biochem. Pharmacol. 31*, 3379–3386.
Herrera, J. E. & Chaires, J. B. (1989) *Biochemistry 28*, 1993–2000.
Huang, Y.-M. & Phillips, D. R. (1977) *Biophys. Chem. 6*, 363–368.
Jin, R., Gaffney, B. L., Wang, C., Jones, R. A., & Breslauer, K. J. (1992) *Proc. Natl. Acad. Sci. U.S.A. 89*, 8832–8836.
Kim, P. S., & Baldwin, R. L. (1990) *Annu. Rev. Biochem. 59*, 631.
Lown, W. J., Sim, S. K., Majumdar, K. C., & Chang, R. Y. (1977) *Biochem. Biophys. Res. Commun. 76*, 705–710.
Manning, G. S. (1983) *Biopolymers 22*, 689–729.
Marky, L. A., & Breslauer, K. J. (1987a) *Biopolymers 26*, 1601–1620.
Marky, L. A., & Breslauer, K. J. (1987b) *Proc. Natl. Acad. Sci. U.S.A. 84*, 4359–4363.
Marky, L. A., Snyder, J. G., Remeta, D. P., & Breslauer, K. J. (1983) *J. Biomol. Struc. Dyn. 1*, 487–507.
Marky, L. A., Curry, J., & Breslauer, K. J. (1985) in *Molecular Basis of Cancer, Part B: Macromolecular Recognition, Chemotherapy, and Immunology* (Rein, R., Ed.) pp 155–173, Liss, New York.
McGhee, J. D. (1976) *Biopolymers 15*, 1345–1375.
Molinier-Jumel, C., Malfoy, B., Reynaud, J. B., & Aubel-Sadron, G. (1978) *Biochem. Biophys. Res. Commun. 84*, 441–449.
Mudd, C. P., & Berger, R. L. (1988) *J. Biochem. Methods 17*, 171–191.
Mudd, C. P., Berger, R. L., Remeta, D. P., & Breslauer, K. J. (1988) *Biophys. J. 53*, 480a.
Nafziger, J., Auclair, C., Florent, J. C., Guillosson, J. J., & Monneret, C. (1991) *Leuk. Res. 15*, 709–13.
Neidle, S., & Taylor, G. L. (1979) *FEBS Lett. 107*, 348–352.
Paar, G. D., & McNulty, H. (1979) *J. Pharm. Pharmacol. 31* (Suppl.), 65.
Patel, D. J., & Canuel, L. L. (1978) *Eur. J. Biochem. 90*, 247–254.
Patel, D. J., Kozlowski, S. A., & Rice, J. A. (1981) *Proc. Natl. Acad. Sci. U.S.A. 78*, 3333–3337.
Phillips, D. R., DiMarco, A., & Zunino, F. (1978) *Eur. J. Biochem. 85*, 487–492.
Pilet, J., Blicharski, J., & Brahms, J. (1975) *Biochemistry 14*, 1869–1876.
Pratt, W. B., & Ruddon, R. W. (1979) *The Anticancer Drugs*, pp 148–194, Oxford University Press, New York.
Pullman, B. (1991) *Anticancer Drug Res. 6*, 95–105.
Quigley, G. J., Wang, A. H.-J., Ughetto, G., van der Marel, G. A., van Boom, J. H., & Rich, A. (1980) *Proc. Natl. Acad. Sci. U.S.A. 77*, 7204–7208.
Remeta, D. P. (1990) Ph.D. Thesis, Rutgers University, New Brunswick, NJ.
Remeta, D. P., Cueto, M. A., & Breslauer, K. J. (1987a) *Abstr. Fifth Conv. Biomol. Stereodynam.* 200–201.
Remeta, D. P., van Hemelryck, B., Gaffney, B. L., Jones, R. A., & Breslauer, K. J. (1987b) *Biophys. J. 51*, 209a.
Remeta, D. P., Mudd, C. P., Berger, R. L., & Breslauer, K. J. (1991) *Biochemistry 30*, 9799–9809.
Ross, W. E., Glaubiger, D. L., & Kohn, K. W. (1979) *Biochim. Biophys. Acta 562*, 41–50.
Scatchard, G. (1949) *Ann. N.Y. Acad. Sci. 51*, 660–672.
Senior, M. M., Jones, R. A., & Breslauer, K. J. (1988) *Proc. Natl. Acad. Sci. U.S.A. 85*, 6242–6246.
Shirley, B. A., Stanssens, P., Hahn, U., & Pace, C. N. (1992) *Biochemistry 31*, 725–732.
Snyder, J. G., Hartman, N. G., D'Estantoit, B. L., Kennard, O., Remeta, D. P., & Breslauer, K. J. (1989) *Proc. Natl. Acad. Sci. U.S.A. 86*, 3968–3972.
Someya, A., & Tanaka, N. (1979) *J. Antibiot. 32*, 839–845.
Vesnaver, G., Chang, C.-N., Eisenberg, M., Grollman, A. P., & Breslauer, K. J. (1989) *Proc. Natl. Acad. Sci. U.S.A. 86*, 3614–3618.
Walter, A. (1985) *Biomed. Biochim. Acta 44*, 1321–1327.
Wang, A. H.-J., Ughetto, G., Quigley, G. J., & Rich, A. (1987) *Biochemistry 26*, 1152–1163.
Wilson, W. D., Wang, Y.-H., Krishnamoorthy, C. R. & Smith, J. C. (1985) *Biochemistry 24*, 3991–3999.
Xodo, L. E., Manzini, G., Ruggiero, J., & Quadrifoglio, F. (1988) *Biopolymers 27*, 1839–1857.
Zunino, F., & Capranico, G. (1990) *Anticancer Drug Res. 5*, 307–317.
Zunino, F., Gambetta, R., DiMarco, A., & Zaccara, A. (1972) *Biochim. Biophys. Acta 277*, 489–498.
Zunino, F., DiMarco, A., Zaccara, A., & Gambetta, R. A. (1980) *Biochim. Biophys. Acta 607*, 206–214.